Bioorganic Chemistry 117 (2021) 105472

Contents lists available at ScienceDirect

Bioorganic Chemistry

journal homepage: www.elsevier.com/locate/bioorg

Design, synthesis and structure-activity evaluation of novel 2-pyridone--based inhibitors of α-synuclein aggregation with potentially improved BBB permeability

Alejandro Mahía [a,b], Samuel Peña-Díaz [c,d], Susanna Navarro [c,d], Juan José Galano-Frutos [b,e], Irantzu Pallarés [c,d], Jordi Pujols [c,d], María D. Díaz-de-Villegas [a,f], José A. Gálvez [a,f,*], Salvador Ventura [c,d,g,*], Javier Sancho [b,e,h,*]

[a] Departamento de Química Orgánica, Facultad de Ciencias, University of Zaragoza, 50009 Zaragoza, Spain
[b] Biocomputation and Complex Systems Physics Institute (BIFI)-Joint Units: BIFI-IQFR (CSIC) and GBsC-CSIC, University of Zaragoza, 50018 Zaragoza, Spain
[c] Departament de Bioquímica i Biologia Molecular, Universitat Autònoma de Barcelona, 08193 Bellaterra, Spain
[d] Institut de Biotecnologia i Biomedicina, Universitat Autònoma de Barcelona, 08193 Bellaterra, Spain
[e] Departamento de Bioquímica y Biología Molecular y Celular, Facultad de Ciencias, University of Zaragoza, 50009 Zaragoza, Spain
[f] Instituto de Síntesis Química y Catálisis Homogénea (ISQCH), CSIC-University of Zaragoza, 50009 Zaragoza, Spain
[g] ICREA, 08010 Barcelona, Spain
[h] Aragon Health Research Institute (IIS Aragón), 50009 Zaragoza, Spain

ARTICLE INFO

Keywords:
Parkinson's disease
Anti-aggregative
Inhibitor
2-Pyridone
BBB permeability
Structure-activity

ABSTRACT

The treatment of Parkinson's disease (PD), the second most common neurodegenerative human disorder, continues to be symptomatic. Development of drugs able to stop or at least slowdown PD progression would benefit several million people worldwide. **SynuClean-D** is a low molecular weight 2-pyridone-based promising drug candidate that inhibits the aggregation of α-synuclein in human cultured cells and prevents degeneration of dopaminergic neurons in a *Caenorhabditis elegans* model of PD. Improving **SynuClean-D** pharmacokinetic/pharmacodynamic properties, performing structure/activity studies and testing its efficacy in mammalian models of PD requires the use of gr-amounts of the compound. However, not enough compound is on sale, and no synthetic route has been reported until now, which hampers the molecule progress towards clinical trials. To circumvent those problems, we describe here an efficient and economical route that enables the synthesis of **SynuClean-D** with good yields as well as the synthesis of **SynuClean-D** derivatives. Structure-activity comparison of the new compounds with **SynuClean-D** reveals the functional groups of the molecule that can be disposed of without activity loss and those that are crucial to interfere with α-synuclein aggregation. Several of the derivatives obtained retain the parent's compound excellent *in vitro* anti-aggregative activity, without compromising its low toxicity. Computational predictions and preliminary testing indicate that the blood brain barrier (BBB) permeability of **SynuClean-D** is low. Importantly, several of the newly designed and obtained active derivatives are predicted to display good BBB permeability. The synthetic route developed here will facilitate their synthesis for BBB permeability determination and for efficacy testing in mammalian models of PD.

1. Introduction

Parkinson's disease (PD) is, after Alzheimer's disease (AD), the second most common neurodegenerative disorder in humans and its incidence is on the rise [1]. PD is highly dependent on age, affecting 1–2% of people older than 65 [2]. Classic symptoms of PD are

Abbreviations: α-syn, α-synuclein; AD, Alzheimer's disease; AUC, area under the curve; BBB, blood-brain barrier; CC50, 50% cytotoxic concentration; CSF, cerebrospinal fluid; IP, intraperitoneal; PD, Parkinson's disease; P-gp, P glycoprotein; PSA, polar surface area; Th-T, Thioflavin-T; TLC, thin-layer chromatography.

* Corresponding authors at: Departamento de Química Orgánica, Facultad de Ciencias, University of Zaragoza, 50009 Zaragoza, Spain (J.A. Gálvez). Departament de Bioquímica i Biologia Molecular, Universitat Autònoma de Barcelona, 08193 Bellaterra, Spain (S. Ventura). Biocomputation and Complex Systems Physics Institute (BIFI)-Joint Units: BIFI-IQFR (CSIC) and GBsC-CSIC, University of Zaragoza, 50018 Zaragoza, Spain (J. Sancho).
E-mail addresses: jagl@unizar.es (J.A. Gálvez), salvador.ventura@uab.cat (S. Ventura), jsancho@unizar.es (J. Sancho).

https://doi.org/10.1016/j.bioorg.2021.105472
Received 3 June 2021; Received in revised form 20 October 2021; Accepted 3 November 2021
Available online 6 November 2021

bradykinesia or slowness of movement, muscle rigidity, resting tremor and postural and gait detriment [3]. In addition, PD patients usually have other non-motor symptoms that negatively affect their quality of life and may lead to cognitive impairment and, finally, dementia in the last stages of the disease [4].

From a physiopathological point of view, PD is characterised by the death of dopaminergic neurons in the midbrain, specifically in the *substantia nigra*, and by the presence of intraneuronal cytoplasmic inclusions named Lewy bodies [5]. Lewy bodies are mainly composed of amyloid fibrils as a result of the aggregation of α-synuclein (α-syn), a 140-amino-acid intrinsically disordered protein whose specific physiological roles are not completely understood [6]. On the other hand, the great variety of genes involved in the evolution of PD, some of which are responsible for the aggregation and proteostasis of α-syn [5,7], highlights the complexity of the pathology and the urgent need to develop novel, precise and effective diagnostic and therapeutic tools.

The therapy currently used to treat PD is a symptomatic treatment based on palliating the symptoms and not acting directly on their molecular mechanisms. Thus, the development of drugs that target the main biomarkers of PD, e.g. the aggregation of α-syn, is a research topic of high interest [8]. In this direction, high-throughput experimental screening methods previously used to discover antimicrobials or aggregation inhibitors [9,10], have been successfully adapted [11] to identify inhibitors of α-syn aggregation [12–14]. Among them, **SynuClean-D** (Fig. 1) stands out. This small metabolically stable 2-pyridone-based compound is not only able to inhibit the aggregation of wild type α-syn and some variants related to familial cases of PD, but also to disrupt pre-formed α-syn fibrils and to avoid aggregate amplification and template seeding processes *in vitro*. Furthermore, **SynuClean-D** reduces α-syn inclusion formation in human neuroglioma cultured cells and prevents degeneration of dopaminergic neurons in a *Caenorhabditis elegans* model of PD [12]. All these properties make **SynuClean-D** a promising chemical scaffold to develop and optimise novel therapeutic compounds for the treatment of PD.

On the other hand, a major challenge in designing drugs targeting the central nervous system (CNS) is to develop molecules able to cross the blood–brain barrier (BBB) and reach optimal concentrations in brain cells [15]. Most CNS drugs are small molecules that cross the BBB by passive diffusion, so the knowledge and purposely optimisation of their physicochemical properties, mainly polarity and lipophilicity, play a crucial role in the design of optimal drug candidates [16].

SynuClean-D was discovered through the screening of a commercially available chemical library. Given the facts that no synthetic procedure has been reported so far to obtain **SynuClean-D**, and that many-gram amounts of this compound are required for pharmacokinetic and pharmacodynamic (PK/PD) assays, and for efficacy testing in mammals, we have developed a synthetic methodology that allows the multi-gram scale synthesis of this molecule in a rapid, efficient and economical manner. Importantly, the designed synthetic strategy can be used for the synthesis of novel derivatives with optimised pharmacological properties. Straightforward assessment of some **SynuClean D** physicochemical features, such as its topological polar surface area (tPSA), suggests that this compound may benefit from rationally improvement in order to increase its BBB permeability [17]. With this purpose, we report the synthesis and *in vitro* efficacy testing of **SynuClean-D** derivatives **6**, **8a-8d** (Fig. 1), **8e-f** and **9** that have been designed to identify the functionalities related to **SynuClean-D** inhibitory activity on α-syn aggregation and to improve its BBB permeation properties.

2. Results and discussion

2.1. Synthesis of SynuClean-D

The synthetic strategy initially designed to obtain **SynuClean-D** is depicted in Scheme 1 and was based on the construction of the 2-pyridone ring through cyclisation between 2-nitro-1,3-dicarbonylic compound **4** and cyanoacetamide as the final step of the reaction sequence. This cyclisation reaction has been previously reported in scientific literature to obtain 3-cyano-6-phenyl-4-trifluoromethyl-2(1*H*)-pyridone (compound **1**) [18,19]. α-Nitro ketone **3** was synthesised from 3-nitrobenzaldehyde in two reaction steps with an overall yield of 81% [20]. However, the synthesis of **4** through acylation of compound **3** did not succeed. Unfortunately, the reaction did not provide the desired 1,3-dicarbonylic compound **4** in any of the reaction conditions tested; ethyl trifluoroacetate or trifluoroacetic anhydride as acylating agents and different basic reagents. This is probably due to the high stability of the enolate of **3**, which leads to a very low or null reactivity. Taking into account these results, a new synthetic strategy in which the heterocyclic nitro group is incorporated to the bicycle scaffold as the final reaction step was designed.

Thus, the synthesis of **SynuClean-D** was attempted by means of the initial construction of the 2-pyridone ring followed by regioselective nitration, as is shown in Scheme 2.

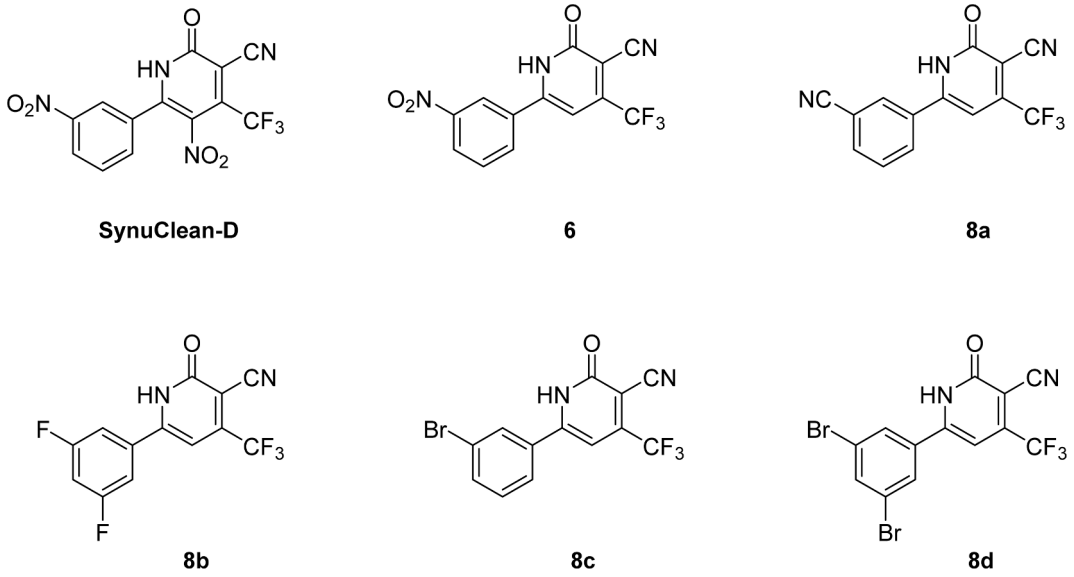

Fig. 1. Chemical structures of **SynuClean-D** and active derivatives with potentially improved BBB permeation.

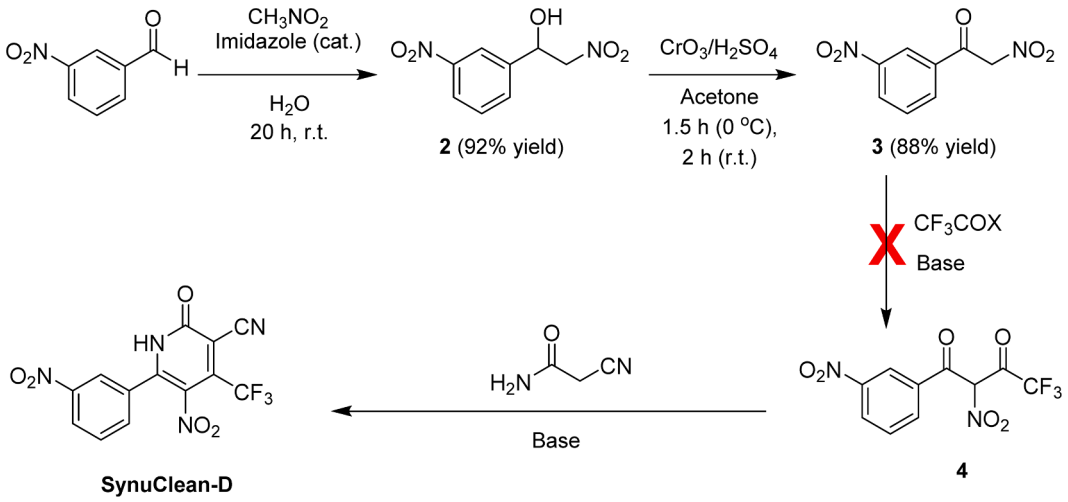

Scheme 1. Initially proposed synthetic route to **SynuClean-D**. The red cross indicates the impossibility of synthesising compound **4** through acylation of **3**.

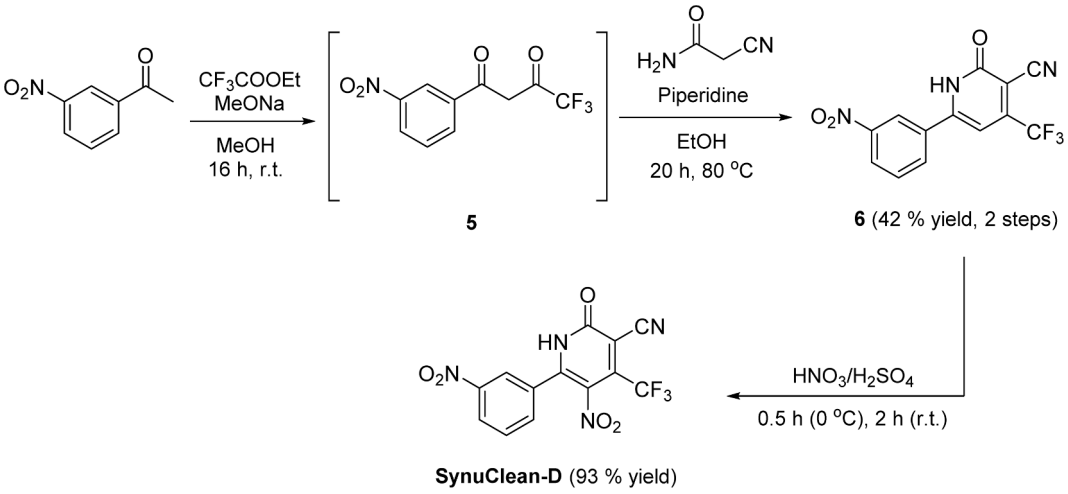

Scheme 2. Successful synthetic route to **SynuClean-D**.

The first step of the synthesis was the acylation of *m*-nitroacetophenone with ethyl trifluoroacetate [21] to obtain 1-trifluoromethyl-1,3-dicarbonylic key intermediate **5**, which was used in the next step without further purification. Compound **6** was obtained through cyclisation reaction between intermediate **5** and cyanoacetamide in the presence of piperidine as catalyst [19], in 42% overall yield for the two steps. The challenge in the synthesis of **SynuClean-D** from compound **6** lies in its regioselective nitration at 5-position of the 2-pyridone ring due to the high number of positions susceptible to be nitrated, which could hinder a clean synthesis of the desired compound. In order to evaluate the chance of the regioselective nitration, we had previously calculated the most nucleophilic position of substrate **6** by two computational methods. The first one, reported by Jørgensen *et al.* in 2016, uses the prediction of ^{1}H NMR and/or ^{13}C NMR chemical shifts to propose the regioselectivity of S_EAr (specially on heteroaromatic systems) in a quick, easy and reliable way using simple computer programs such as ChemDraw [22]. This method is based on the fact that the position with the lowest chemical shift will be that with more electron density and, consequently, more prone to the electrophilic attack. ^{1}H NMR and ^{13}C NMR chemical shifts predicted by ChemDraw for compound **6** are collected in Fig. 2. As can be observed, the lowest value in both cases was obtained for the 5-position of the 2-pyridone ring, what indicates that the synthesis of **SynuClean-D** by regioselective nitration of compound **6** might be viable. Besides, the real ^{1}H NMR spectrum of **6**

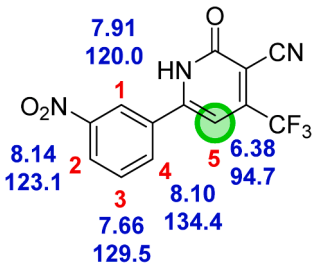

Fig. 2. Computational predictions for the regioselectivity nitration of compound **6**. The values of ^{1}H NMR and ^{13}C NMR chemical shifts predicted by ChemDraw for compound **6** are shown in blue. The green circle indicates the most reactive aromatic position of **6** (in S_EAr reactions) predicted by RegioSQM online tool.

also showed the lowest chemical shift on that position. More recently, RegioSQM has been reported by the same authors as a novel, accurate and free-access computational tool to predict the regioselectivity of S_EAr reactions [23]. RegioSQM is based on semiempirical quantum mechanical (SQM) methods that predict the arenium ion with lowest free energy and, therefore, the most reactive position. When RegioSQM

computational tool was tested with compound **6**, the 5-position of the 2-pyridone cycle was predicted again as the most reactive (Fig. 2), providing new evidence on the feasibility of synthesising **SynuClean-D** by regioselective nitration of **6**. In effect, the nitration of **6** in the presence of nitric acid and sulphuric acid at low temperature [24] afforded **SynuClean-D** as the sole reaction product with an excellent yield of 93% (Scheme 2). This result confirmed the goodness of the assayed predictive computational methods for our particular issue.

Therefore, an efficient and inexpensive synthetic procedure has been developed that allows us to obtain **SynuClean-D** in as few as three steps with a global yield of 39%. Furthermore, this methodology offers the possibility of synthesising novel derivatives of **SynuClean-D** by varying substituents at different positions. By comparing the anti α-syn aggregation activity of **SynuClean-D** and derivatives so synthesised we have identified structural determinants of **SynuClean-D** inhibitory activity as well as introduced functionalities that may increase the BBB permeability of the parent compound (see below).

2.2. SynuClean-D concentration in cerebrospinal fluid (CSF) and in plasma. Computational prediction of BBB permeability

To preliminarily examine **SynuClean-D** BBB permeability, its pharmacokinetic profile was evaluated. Table 1 summarises the pharmacokinetic parameters for **SynuClean-D** in plasma and cerebrospinal fluid (CSF).

According to the obtained results, **SynuClean-D** mean concentration in CSF is significantly lower than in plasma (Fig. 3): C_{max} values of 30.9 ng/mL and 44.2 μg/mL, respectively. A terminal elimination half-life ($T_{1/2}$) of 3.6 h and 3.4 h was determined in plasma and CSF, respectively. The T_{max} in plasma and CSF was reached in both cases 0.5 h after intraperitoneal (IP) administration, and **SynuClean-D** concentrations were quantifiable for up to 24 h post-dosing in plasma and 6 h in CSF. The CSF exposure (96.7 h•ng/mL) was very low compared with plasma (372.8 h•μg/mL). The Ratio CSF/plasma calculated by means of the AUCs was 0.0003 (0.03%). Although this low CSF/plasma ratio could arise – in principle – from very intense **SynuClean-D** uptake by plasma proteins or by brain tissue, or even from very active efflux of **SynuClean-D** molecules after having crossed the BBB, it suggests that **SynuClean-D** may have a low BBB penetration.

To further investigate this possibility we have obtained a consensus computational evaluation of **SynuClean-D** BBB crossing potential using three web servers based on different models. *BOILED-Egg* predicts the passive gastrointestinal absorption and BBB permeation of small organic molecules, from their lipophilicity (octanol–water partition coefficient: logP) and polarity (polar surface area: PSA) [25]. This model computes and graphically represents lipophilicity versus polarity of the studied compound. In the generated plot the compound may lay in one of three regions: the outer one corresponding to compounds that are not even absorbed by the gastrointestinal tract, the white area of the egg-shaped diagram corresponding to compounds absorbed but unable to cross efficiently the BBB, and the yolk area, for those that are expected to cross the barrier. **SynuClean-D** locates in the outer region (Fig. 4) and is – therefore – predicted as displaying a poor gastrointestinal absorption and being unable to cross the BBB. *AlzPlatform* [26] is another free-access server whose BBB predictor provides, for the input molecule, a BBB crossing prediction based on a support vector machine algorithm that uses four types of fingerprints (mainly hydrogen bond-related properties of the molecule) [27]. The BBB crossing prediction for **SynuClean-D** is also negative. On the other hand, the BBB predictor from the *VEGA suite* [28] is a free-access server based on a decision tree model built through machine learning that uses nine attributes of the input molecule related to size, shape, charge, lipophilicity and Kier-Hall E-state descriptors. The BBB crossing prediction of this server for **SynuClean-D** is also negative. Thus, three different predictors using different models provide a clear consensus prediction indicating that the BBB permeability of **SynuClean-D** is low and, therefore, it is unable to significantly cross the BBB.

We have used the *P-gp substrate* prediction module in *SwissADME* [29] to evaluate whether a very active efflux of **SynuClean-D** from CSF associated to the activity of P glycoprotein could contribute to the very low CSF/plasma concentration ratio observed. This seems unlikely as the *P-gp substrate* module predicts that **SynuClean-D** does not interact with P glycoprotein. The possibility that a very high plasma protein or brain tissue binding of **SynuClean-D** could contribute to the very low observed CSF/plasma concentration ratio cannot be discarded yet.

Table 1
Pharmacokinetic parameters of **SynuClean-D** in plasma and CSF following an intraperitoneal single dose 10 mg/kg in male Wistar rats.[a]

	T_{max} (h)	C_{max} (ng/mL)	AUC_{last} (h•ng/mL)	$T_{1/2}$ (h)	CSF to plasma exposure ratio
Plasma	0.5	44 230	372 820	3.6	0.03%
CSF	0.5	30.9	96.7	3.4	

[a]Mean concentration values were used for calculation of pharmacokinetic parameters.

2.3. Computational design and synthesis of novel derivatives of SynuClean-D with predicted better membrane permeability

We have used *BOILED-Egg*, and the BBB crossing predictors in *AlzPlatform* and in the *VEGA suite* to guide the design of **SynuClean-D** derivatives. On one hand, the derivatives have been designed to provide an opportunity to dissect the contribution of **SynuClean-D** functionalities to its inhibitory activity on α-syn aggregation and, on the other, to improve their predicted BBB permeability.

A quick inspection of the *BOILED-Egg* graph (Fig. 4) indicates that the membrane permeation of **SynuClean-D** could be easily improved by reducing its PSA. This can be achieved e.g. through the elimination of the phenyl-nitro group and/or heterocyclic nitro group in **SynuClean-D** or through their replacement by other less polar substituents such as nitrile or halogen functional groups. In addition, the generation of 1*N*-methylated derivatives of **SynuClean-D** can also reduce its PSA. In this respect, the synthetic strategy followed to obtain **SynuClean-D** enabled the synthesis of derivatives **1**, **6** and **8a-f** with expected moderate yields in only two reaction steps starting from different ring-substituted acetophenones or employing a *N*-methylated cyanoacetamide (Scheme 3 and Table 2).

The nitration of compound **8f** under the same conditions as those applied to **6** afforded dinitrated compound **9** in a regioselective manner and with a very good yield of 72% (Scheme 4). As well as for **SynuClean-D**, the synthesis of compounds **6**, **8a**, **8b**, **8c**, **8d**, **8f** and **9** is being reported for the first time.

With the exception of dinitrated compound **9**, all these newly obtained derivatives are located in the *BOILED-Egg* graph (Fig. 4) in a region with good predicted membrane permeability, all of them offering better polarity parameters and similar or better lipophilicity than **SynuClean-D**. Additionally, some of them are located inside the region with high probability to permeate across the BBB.

The BBB permeability predictors in *AlzPlatform* and in the *VEGA suite* are binary. They classify compounds as BBB+ or BBB-, not providing indications of their gastrointestinal absorption. These two servers classify **SynuClean-D** as BBB-, compound **9** as BBB- (*AlzPlatform*) or BBB+ (*VEGA suite*), and all the other derivatives as BBB+. The qualitative agreement between the three servers is good as it coincides in the poor BBB permeability of **SynuClean-D**, and its significant improvement in all the derivatives synthesised with the possible exception of derivative **9**.

2.4. Anti-aggregative activity of the obtained SynuClean-D derivatives

The inhibitory effect of **SynuClean-D** on the aggregation of α-syn *in*

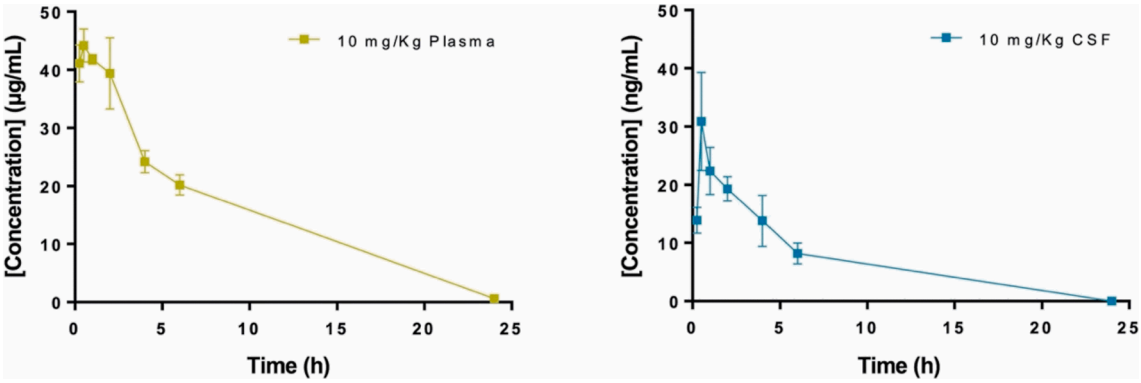

Fig. 3. Plasma and CSF concentration *vs* time for **Synuclean-D** (10 mg/kg, IP) in rat. Plasma and CSF samples were collected at 0, 0.25, 0.5, 1, 2, 4, 6 and 24 h post-dosing, three Wistar male rats per time point were assessed. 3 rats were not administered and referred as t = 0. The values represent mean ± SEM (n = 3).

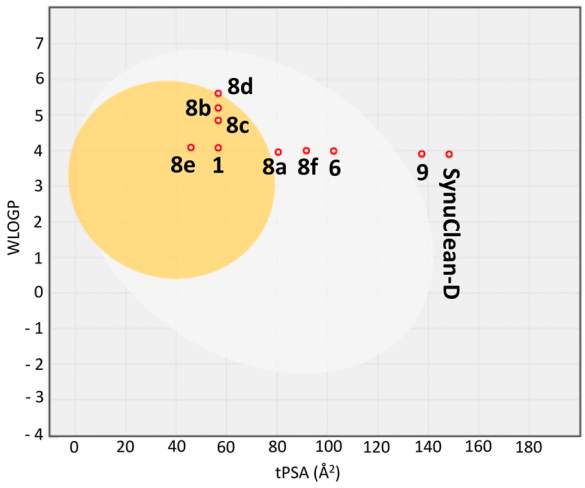

Fig. 4. BOILED-Egg graph for compounds **1**, **6**, **8a-f**, **9** and **SynuClean-D**. SwissADME free web tool was used for graphic representation of lipophilicity (WLOGP) and polarity (tPSA) computationally obtained values [29].

vitro has been carefully analysed previously [11]. It can be conveniently monitored as an attenuation of the Thioflavin-T (Th-T) fluorescence increase observed upon α-syn aggregation in absence of inhibitor. **SynuClean-D** alone does not quench or absorb Th-T emission fluorescence and the inhibition observed using Th-T has been thoroughly validated using transmission electron microscopy (TEM). TEM analysis indicates that α-syn aggregation in presence of **SynuClean-D** takes place with an important decrease in both number and size of α-syn fibrils [11]. In order to assess whether **SynuClean-D** modifications intended to improve its BBB permeability impact its anti-aggregative capacity we have assayed the derivatives using the same protocol implemented to discover **SynuClean-D** and the active **ZPD-2** and **ZPDm** molecules [11–14].

This protocol attains the formation of α-syn amyloid fibrils *in vitro* in a ~ 30 h reaction, and uses Th-T fluorescence as a readout for the presence of these structures (Fig. 5). The incubation of 70 µM of recombinant α-syn in the presence and absence of 100 µM of the different **SynuClean-D** derivatives revealed that compound **8e** has lost any anti-aggregative activity and compound **1** has turned into a pro-aggregative molecule. The rest of compounds could be ranked into three groups according to their activity: (**8b** and **8c**) > (**6** and **8d**) > (**8a** and **8f** and **9**). Remarkably, the anti-aggregative activity of the first two groups is comparable to that of **SynuClean-D** (Fig. 5, Fig. S1 and Table S1).

2.5. Cellular toxicity of SynuClean-D derivatives

The structural modifications introduced in **SynuClean-D** derivatives may impact their toxicity in human cells. This effect was assayed in the MRC-5 (non-tumor human lung fibroblast) cell line at the **SynuClean-D** concentration shown to be neuroprotective (10 µM) [12], and at 5- and 10-fold this concentration. All the molecules were innocuous at 10 µM, except compound **8d** which allowed for a 80% cellular viability at this concentration. At the high 100 µM concentration, all compounds

Table 2
Synthesis of derivatives of SynuClean-D (1, 6, 8a-f) with different substituents by adapting the designed synthetic route.

SynuClean-D derivative	R_1	R_2	R_3	Yield (%)
1	H	H	H	75
6	NO_2	H	H	42 (2 steps)
8a	CN	H	H	23 (2 steps)
8b	F	F	H	46 (2 steps)
8c	Br	H	H	51 (2 steps)
8d	Br	Br	H	38 (2 steps)
8e	H	H	Me	65
8f	NO_2	H	Me	36 (2 steps)

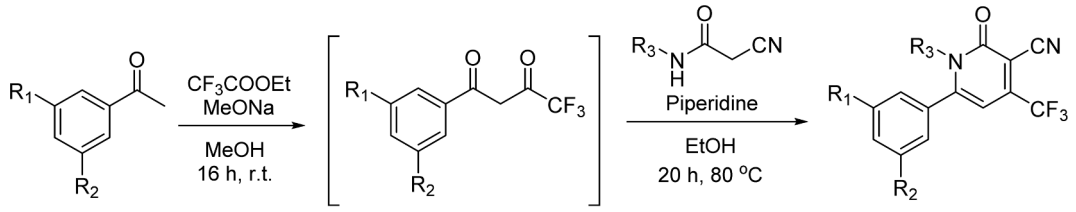

Scheme 3. Successful synthetic route to **SynuClean-D** derivatives: **1**, **6**, **8a-f**.

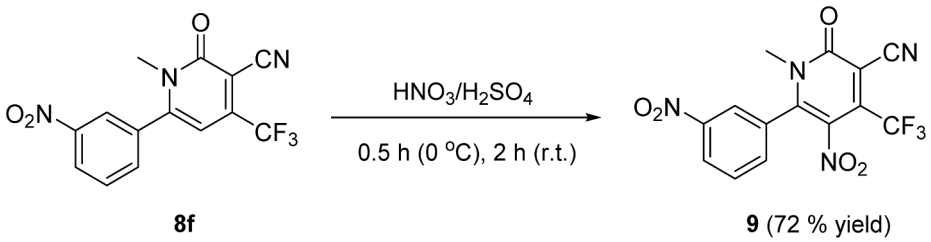

Scheme 4. Regioselective nitration of compound **8f**.

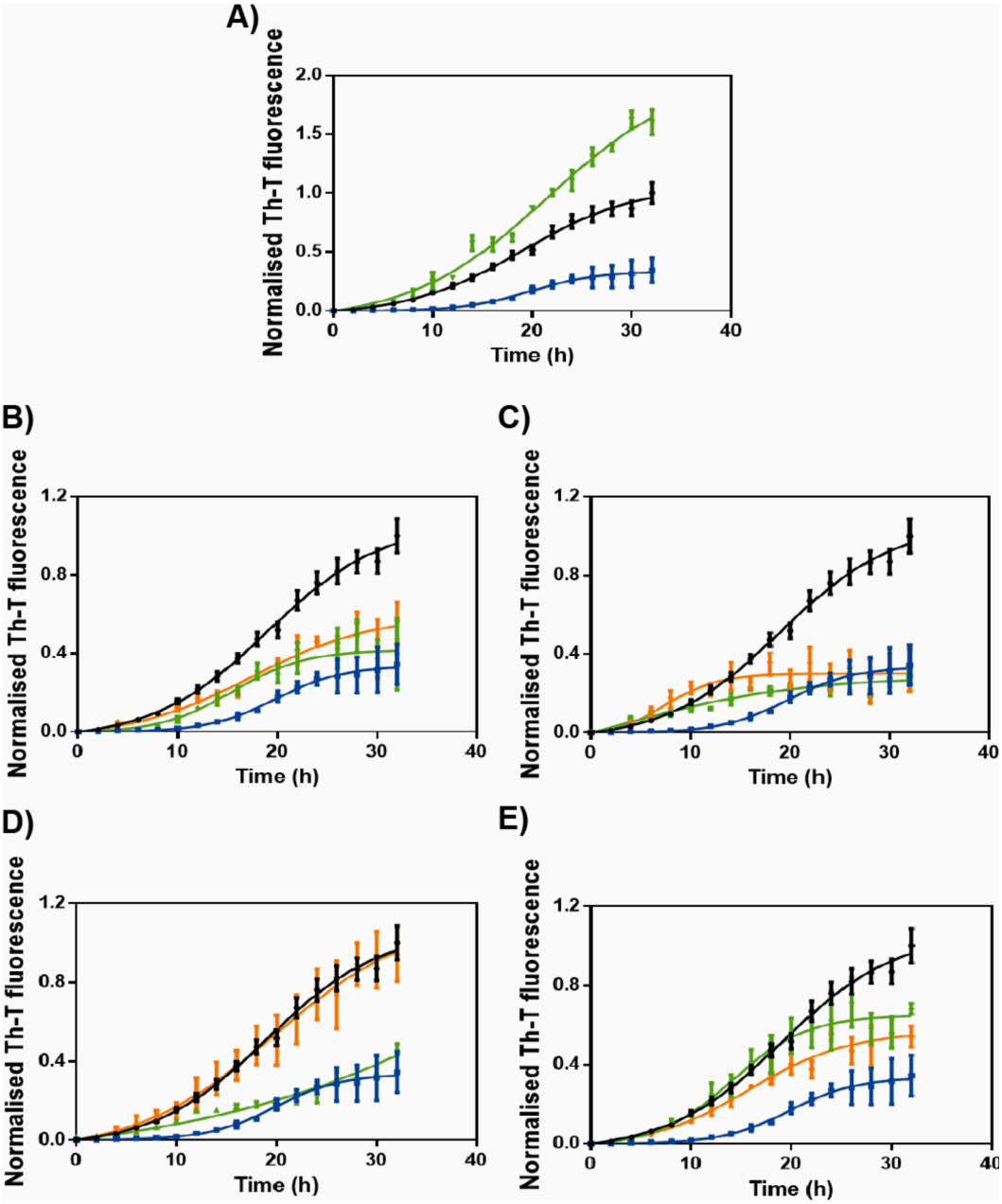

Fig. 5. *In vitro* analysis of the inhibitory capacity of **SynuClean-D** derivatives. α-syn aggregation kinetics followed by Th-T–emitted fluorescence in the absence (black) and presence of **SynuClean-D** (blue), and (A) derivative **1** (green), (B) derivatives **6** (green) and **8a** (orange), (C) derivatives **8b** (green) and **8c** (orange), (D) derivatives **8d** (green) and **8e** (orange), and (E) derivatives **8f** (green) and **9** (orange). Th-T fluorescence is plotted as normalised means and error bars are represented as SE of mean values.

allowed for at least 80% cell viability, except compounds **8b** and **8d**. Thus, only the compounds containing either two fluorine (**8b**) or two bromine atoms (**8d**) were significantly toxic at the highest concentration (Fig. 6).

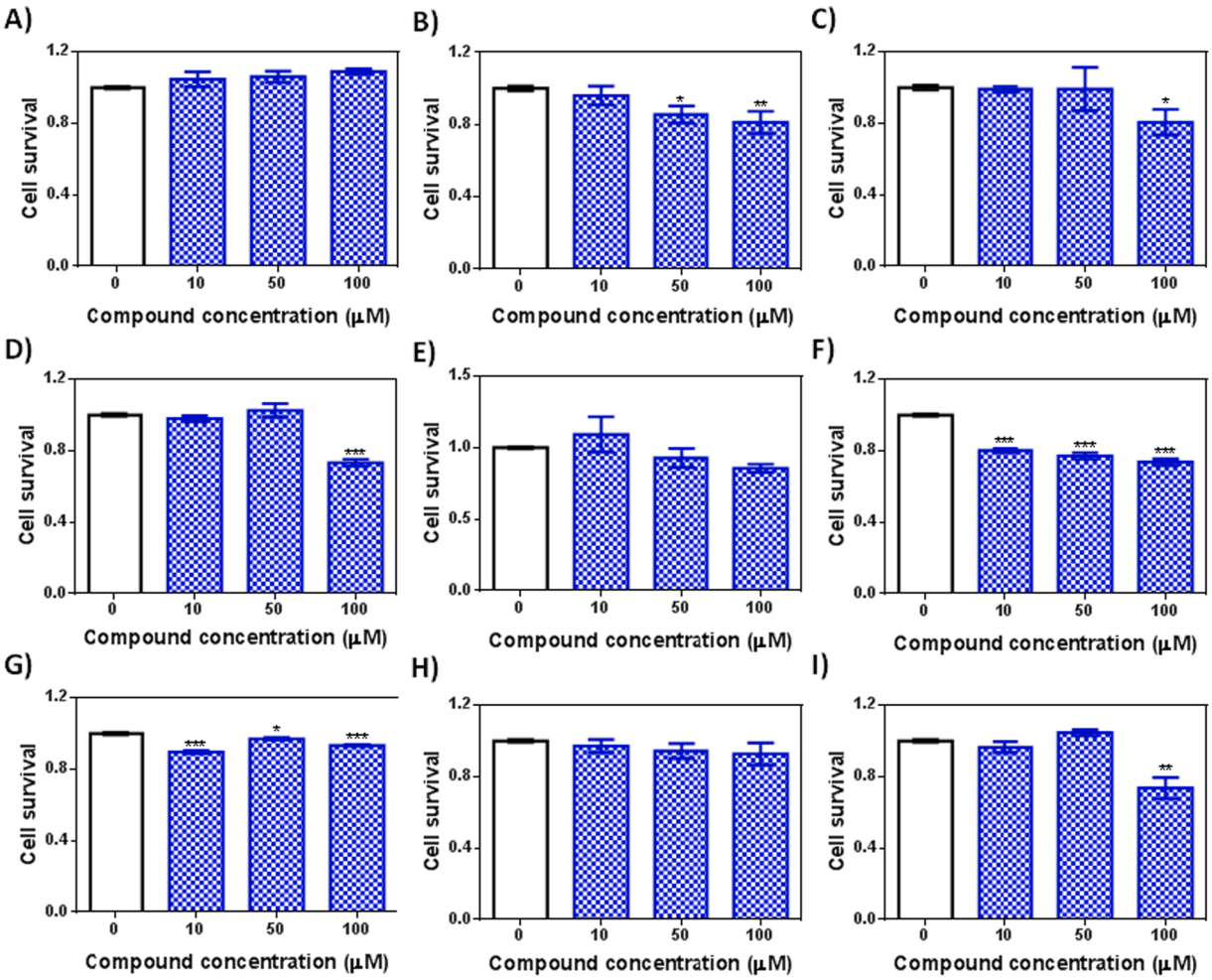

Fig. 6. Toxicity of **SynuClean-D** derivatives in MRC-5 cell cultures. Normalised MRC-5 cell survival in presence of different concentrations of compound **1** (A), **6** (B), **8a** (C), **8b** (D), **8c** (E), **8d** (F), **8e** (G), **8f** (H) and **9** (I). Survival is plotted as normalised means. Error bars are shown as standard error of means values, where $p < 0.05$, $p < 0.01$ and $p < 0.001$ were indicated by *, ** and *** respectively.

2.6. Structure-activity insights from comparison of SynuClean-D and derivatives' in vitro efficacies

Qualitatively, the above results indicate that the ability of **SynuClean-D** to inhibit the amyloid aggregation of α-syn *in vitro* is strongly influenced by the absence or presence of some of its functional groups (Figs. 5 and S1). For example, the lack of activity found for non-nitrated compound **1** compared to the activity of mononitrated compound **6** and dinitrated **SynuClean-D** indicates that the phenyl-nitro group, unlike the heterocyclic one, plays an important role in keeping the anti-aggregative activity of the compounds. In fact, non-nitrated compound **1** promotes rather than inhibits α-syn aggregation. On the other hand, compounds **8e**, **8f** and **9** are 1*N*-methylated derivatives of compounds **1**, **6** and **SynuClean-D**, respectively. These 1*N*-methylated analogues display a reduced PSA compared to the non-methylated corresponding ones, which brings them closer to the yellow ellipse in the graphic *BOILED-Egg* representation (Fig. 4). Unfortunately, 1*N*-methylation, which locks the amide-iminol equilibrium of the non-methylated compounds in the amide form, significantly reduces the compounds' anti-aggregation activity. The amide-iminol region of **SynuClean-D** may play a significant role in the recognition of α-syn aggregates. Actually, the aggregation kinetics of the non-nitrated and 1*N*-methylated compound **8e** cannot be distinguished from control kinetics, suggesting the compound doesn't bind to α-syn or its aggregates. Another way to decrease the PSA of **SynuClean-D**, thus potentially improving its membrane permeability, is by replacing nitro groups with other less polar substituents. While the heterocyclic nitro group can be removed without significant activity loss, the phenyl-nitro has to be judiciously replaced. A comparison between nitro compound **6** and nitrile **8a** shows that the bioisosteric replacement of the phenyl-nitro by a cyano group retains most of the anti-aggregation activity of compound **6**. Neither compound **6** nor **8a** have shown toxicity against MRC-5 cells in our assay (Fig. 6). However, nitro aromatic compounds are not infrequently associated with toxicity problems *in vivo* [30] and, in this respect, compound **8a** constitutes an interesting similarly active alternative to nitro compound **6**. The non-isosteric substitution of the phenyl-nitro group by halides enables to bring **SynuClean-D** derivatives into the BBB permeation area within the *BOILED-Egg* graph (Fig. 4). Compound **8c**, bearing a bromine atom at meta position on the benzene ring, exhibits an anti-aggregation activity similar to that of **SynuClean-D**. Incorporating a second bromine atom at the other meta position in compound **8d** slightly reduces the activity. Finally, compound **8b**, where the bromine atoms in **8d** are replaced by fluorine, slightly improves the *in vitro* anti-aggregative activity of **SynuClean-D**. While compounds **8b** and **8d** may be more toxic towards MRC-5 cells than **SynuClean-D**, their CC50 are still > 100 μM. Importantly, **SynuClean-D** displays its neuroprotective effect at 10 μM, a concentration at which compounds **8b** and **8c** are not toxic. Taken together, the anti-aggregative activity of **SynuClean-D** and tested derivatives points to an important role of the amide-iminol group in the recognition of α-syn aggregates and of electron-withdrawing groups at meta position of the phenyl ring in the anti-aggregative activity.

As a classical QSAR modeling is not suitable for such a small compound series here shown, a simple structure–activity analysis has been performed to obtain the individual contribution to the aggregative inhibitory potency of the functional groups added to or removed from **SynuClean-D**. The analysis performed is described in Section 4.6 and the results obtained are summarized in Table 3 and Fig. 7.

Positive contributions are obtained for all the electron-withdrawing functional groups added/removed both in the phenyl and 2-pyridone rings, except for the simultaneous addition of two bromines in the phenyl ring. A modest contribution (0.09/0.10) is provided by a nitro group at position 5 of the heterocyclic ring. At position 3 of the phenyl ring, nitro and cyano groups make larger contributions of 0.31/0.32 and 0.22, respectively. The highest positive contribution at this position is made by bromine: 0.44 (derivative **8c)**. However, incorporation of a second bromine at position 5 (derivative **8d**) brings about a negative contribution: −0.14, making the compound with two bromines less active than that with one. Interestingly, the simultaneous incorporation of two fluorine atoms at positions 3 and 5 of the phenyl ring (derivative **8b**) comes with a combined positive contribution of 0.48, which is the highest observed in the series. In contrast, a detrimental negative contribution of –0.22 is obtained for the methyl group placed on the nitrogen of the 2-pyridone ring (compounds **8e**, **8f** and **9**).

3. Conclusions

SynuClean-D, a potent inhibitor of α-syn aggregation that protects against α-syn induced dopaminergic neurons damage in cellular and animal models, can be efficiently synthesised in gr-amounts using an economical route that also enables the synthesis of **SynuClean-D** derivatives. The BBB permeability of **SynuClean-D** appears to be low. Using the synthetic route, new derivatives have been synthesised and tested that retain the anti-aggregative activity and low toxicity of **SynuClean-D** and are predicted to display better BBB permeability. Structure-activity comparisons have allowed us to identify specific functionalities in the **SynuClean-D** molecule that are particularly important for its biological activity, and others that can be removed without activity loss. These findings will facilitate designing, synthesising and testing even more active variants.

4. Experimental section

4.1. Animals and treatments

Animal care, including environmental and housing conditions conformed to the applicable Standard Operating Procedures regarding laboratory animals of *Draconis Pharma S.L. (Barcelona, Spain)*. Animal experimental procedures were approved by the Animal Experimentation Ethical Committee of Universitat Autònoma de Barcelona (procedure number: 3967) and by Catalan Government Experimentation Commission Board. The animals were maintained and used in accordance with the National rules and the European Community Council Directive (86/609/EEC) for the care and handling of laboratory animals.

4.2. Plasma and brain distribution of SynuClean-D

Analysis of **SynuClean-D** exposure in plasma and brain was conducted by *Draconis Pharma S.L.* BBB permeability studies to evaluate the plasma and brain distribution of **SynuClean-D** were measured as

Table 3
Quantitative structure-activity analysis for evaluating the individual contribution of functional groups added to or removed from SynuClean-D.

Cp	Change	Sub-structure 1[a]	Sub-structure 2[a]	Effect upon change[b]	Effect breakdown[c]	Quantitative effect
1	Removed	–NO_2 (–x)	–NO_2 (–y)	–1.30	–x + (–y) = –1.30 **(Eq. (1))**	Outlier[d]
	Added	-	-			
6	Removed	-	–NO_2 (–y)	–0.09	–y = –0.09 **(Eq. (2))**	y = 0.09
	Added	-	-			
8a	Removed	–NO_2 (–x)	–NO_2 (–y)	–0.21	–x + z + (–y) = –0.21 **(Eq. (3))**	z = 0.20[e]
	Added	–CN (z)	-			
8b	Removed	–NO_2 (–x)	–NO_2 (–y)	0.07	–x + 2w + (–y) = 0.07 **(Eq. (4))**	w = 0.24[e]
	Added	2 x –F (w)	-			
8c	Removed	–NO_2 (–x)	–NO_2 (–y)	0.03	–x + v_1 + (–y) = 0.03 **(Eq. (5))**	v_1 = 0.44[e]
	Added	–Br (v_1)	-			
8d	Removed	–NO_2 (–x)	–NO_2 (–y)	–0.11	–x + v_1 + v_2 + (–y) = –0.11 **(Eq. (6))**	v_2 = –0.14[e]
	Added	2 x –Br (v_2)	-			
8e	Removed	–NO_2 (–x)	–NO_2 (–y)	–0.63	–x + u + (–y) = –0.63 **(Eq. (7))**	x = 0.32 (0.31)[f]
	Added	-	–CH_3 (u)			
8f	Removed	-	–NO_2 (–y)	–0.32	u + (–y) = –0.32 **(Eq. (8))**	y = 0.10[g]
	Added	-	–CH_3 (u)			
9	Removed	-	-	–0.22	u = –0.22 **(Eq. (9))**	u = –0.22
	Added	-	–CH_3 (u)			

[a]Sub-structure 1 corresponds to the phenyl ring whereas sub-structure 2 corresponds to the heterocyclic ring in SynuClean-D derivatives.
[b]Obtained by subtracting SynuClean-D's aggregative inhibitory potency (Table S1 and Fig. S1) from those of the derivatives.
[c]The effect upon change (functional group added or removed) relying on the individual contributions of the functional groups added/removed. The contribution of the moiety is assumed to be positive when it is added to any sub-structure and negative when it is removed.
[d]Effect upon change for compound 1 considered as atypical (outlier) so that Eq. (1) was not used in the calculation of the quantitative contributions.
[e]Obtained by solving the corresponding Eq. with y being 0.09 (Eq. (2)) and x being 0.32 (Eq. (7)). To solve Eq. (6) the value of v1 used is that obtained from solving Eq. (5). Any other combination of values used (e.g. y = 0.1, x = 0.31) will lead to very similar results.
[f]Value of 0.32 obtained for x (–NO_2 in sub-structure 1) by solving Eq. (7) with y being 0.09 (Eq. (2)) and u being −0.22 (Eq. (9)). Between parentheses the value obtained for x if used y = 0.1 as obtained from Eq. (8).
[g]Obtained by solving Eq. (8) with u being −0.22 (Eq. (9)).

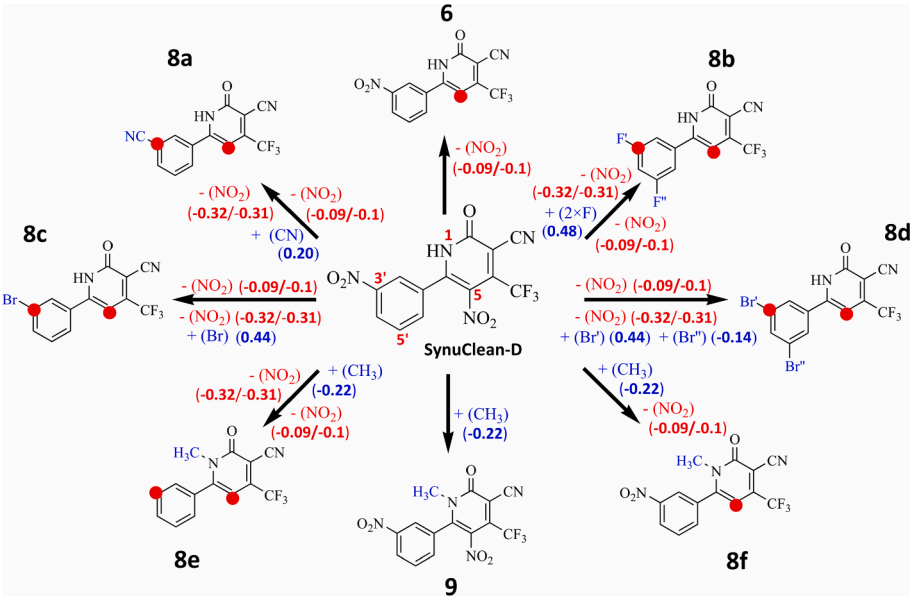

Fig. 7. Individual contribution of functional groups to the aggregative inhibitory activity in a **SynuClean-D** derivatives series. Removed (highlighted in red and preceded by a '−' sign) and added (highlighted in blue and preceded by a '+' sign) functional groups are indicated close to the thick arrows. Changes occurring in the phenyl ring are placed at the arrows' left or below, and those occurring in the heterocyclic ring at their right or above. Groups' individual quantitative contributions are indicated with the same color code. Positive values enhance the aggregative inhibitory potency and negative values decrease it.

comparison of cerebrospinal fluid (CSF) levels and plasma levels and were performed after 10 mg/kg **SynuClean-D** intraperitoneal (IP) administration. The administered volume was 10 mL/kg. Plasma and CSF samples were collected at 0, 0.25, 0.5, 1, 2, 4, 6 and 24 h post-dosing and three rats per time point were assessed (Wistar rats (HsdHanWIST), 125–150 g approx.). Three rats were not administered and referred as t = 0. CSF samples were collected from cisterna magna in anesthetised animals. Samples contaminated with blood were discarded and not included in the analysis. The samples were stored at −20 °C until analysis. Blood samples (0.5–0.8 mL) were collected from anesthetised animals with isoflurane by cardiac puncture, in tubes containing K2-EDTA 5%. Blood samples were centrifuged at 10 000 rpm for 5 min to obtain plasmas that were stored at −20 °C until analysis. Analytical measurements were performed by liquid chromatography-tandem mass spectrometry (LC-MS/MS). The calibration curves were conducted using blank rat plasma and artificial rat blank CSF. The lowest standard concentration on the calibration curve was 8.82 ng/mL for plasma and 4.42 ng/mL for CSF. Pharmacokinetic parameters were calculated with Phoenix 64 8.1 (*WinNonlin*).

4.3. Inhibition of in vitro α-synuclein aggregation by SynuClean-D derivatives

α-syn expression and purification were performed in *Escherichia coli BL21 DE3* strain as previously described[11]. The obtained protein was lyophilised and stored at −80 °C until employed. The aggregation of α-syn was carried out in a 96-well sealed plate. Each well contained 70 μM α-syn in PBS 1X, 40 μM Th-T, a 1/8-inch diameter teflon polyball (*Polysciences Europe GmbH, Eppelheim, Germany*) and 100 μM of **SynuClean-D**, its derivatives, or the corresponding amount of DMSO as a control, in a final volume of 150 μL. The plate was steadily agitated at 100 rpm and 37 °C, fixed into an orbital Max-Q 4000 (*ThermoScientific, Waltham, Massachusetts, USA*). Th-T fluorescence was measured every 2 h by exciting through a 430–450 nm filter and collecting the emission signal with a 480–510 filter, using a TECAN Spark (*Tecan Trading AG, Switzerland*). All assays were performed in triplicate. Data was normalised and represented as mean and standard error of mean (SEM), and fitted with GraphPad Prism 6.0 software (*GraphPad Software Inc., La Jolla, California, USA*) by using Eq. (10):

$$\propto = 1 - \frac{1}{k_b(e^{k_a t} - 1) + 1} \tag{10}$$

where k_b and k_a account for the homogeneous nucleation rate constant and the secondary rate constant, respectively [31].

4.4. Toxicity assays of SynuClean-D derivatives

MRC-5 cells (ATCC CCL-171) were cultured in DMEM (*Gibco*) supplemented with 10% fetal bovine serum at 37 °C in a 5% CO_2 humidified incubator in 75 cm^3 tissue culture-treated flasks. Cells were plated at a concentration of 3500 cells/well in 96-well plates in full medium and incubated at 37 °C overnight. Then cells were treated with the **SynuClean-D** derivatives at concentrations 10, 50 and 100 μM for 72 h, in triplicates. In controls, the equivalent amount of DMSO relative to each concentration of compound diluted in PBS was added. Treated cells were incubated with 10 μL PrestoBlue® Cell Viability Reagent (*ThermoFisher Scientific, Waltham, MA, United States*) for 15 min. Cell viability was determined recording fluorescence at 615 nm, with an excitation wavelength of 531 nm in a Victor3 Plate reader (*Perkin Elmer, USA*).

4.5. Chemistry

Unless otherwise specified, all reagents were obtained from commercial suppliers and were used without purification. TLC was performed on precoated silica gel polyester plates, and products were visualised using UV light (254 nm) and ninhydrin, anisaldehyde, or potassium permanganate solutions followed by heating. Column chromatography was performed on silica gel 60 (70–200 μm) with air pressure. Melting points were determined in open glass capillaries with a Gallenkamp apparatus. Infrared spectra were recorded with a Fourier transform infrared spectrometer (Nicolet Avatar 360 FT-IR). NMR spectra were recorded with a Bruker AV400 spectrometer (400 MHz for ^{1}H NMR experiments, 100 MHz for ^{13}C NMR experiments and 376 MHz for ^{19}F NMR experiments) in the stated deuterated solvents. ^{1}H and ^{13}C chemical shifts were referenced to internal solvent resonances and reported in ppm relative to tetramethylsilane. *J* values are given in Hz. High-resolution positive (or negative) electrospray ionisation mass spectra were recorded with a Bruker Daltonics MICROTOF-Q spectrometer with use of ultradilute solutions of the chemical compounds in methanol. All compounds used for biological assays are of ≥ 95% purity based on elemental analysis (found values are within ± 0.4% of the calculated values).

2-Oxo-6-phenyl-4-(trifluoromethyl)-1,2-dihydropyridine-3-carbonitrile ***(1)*** . To a mixture of benzoyl-1,1,1-trifluoroacetone (1.73 g, 8.00 mmol)

and cyanoacetamide (673 mg, 8.00 mmol) in ethanol (8.0 mL), piperidine (79 μL, 0.80 mmol) was added and the resulting suspension was refluxed for 7 h. The reaction mixture was allowed to cool at room temperature and the precipitate was collected by filtration, washed with cold ethanol (8 mL) and dried under vacuum to afford compound **1** (1.58 g, 75% yield) as a yellow solid. **Mp**: 305–306 °C. **IR** (KBr, ν_{max}/cm^{-1}): 1653, 2228. **^{1}H NMR** (400 MHz, DMSO-d_6, δ): 7.96 (d, 2H, J = 7.2), 7.65–7.51 (m, 3H), 7.24 (br s, 1H). **^{13}C NMR** (100 MHz, DMSO-d_6, δ): 162.3, 156.1, 145.2, 132.5, 131.8, 129.0, 128.0, 121.3 (q, J = 274), 113.4, 109.3, 102.7. **^{19}F NMR** (376 MHz, DMSO-d_6, δ): −63.4. **HRMS** (ESI^+): *m/z* $[M + Na]^+$ calculated for $C_{13}H_7F_3N_2NaO$ 287.0403, found 287.0406.

*2-Nitro-1-(3-nitrophenyl)ethan-1-ol (**2**)*. A mixture of 3-nitrobenzaldehyde (786 mg, 5.20 mmol), nitromethane (0.85 mL, 15.6 mmol) and imidazole (90 mg, 1.32 mmol) in distilled water (10 mL) was stirred at room temperature for 20 h. The reaction mixture was extracted with dichloromethane (2 × 10 mL). The combined organic phases were dried with anhydrous $MgSO_4$, filtered and evaporated under reduced pressure. The resulting residue was purified by column chromatography (eluent 1: hexane/Et_2O 3:2, eluent 2: hexane/Et_2O 1:1) to afford compound **2** (1.02 g, 92% yield) as a white solid. **Mp**: 76–77 °C. **IR** (KBr, ν_{max}/cm^{-1}): 1350, 1525, 1551, 3492. **^{1}H NMR** (400 MHz, $CDCl_3$, δ): 8.33–8.28 (m, 1H), 8.20 (ddd, 1H, J = 8.0, J = 2.0, J = 0.8), 7.80–7.44 (m , 1H), 7.60 (dd, 1H, J = 8.0, J = 8.0), 5.61 (dd, 1H, J = 8.2, J = 4.2), 4.64 (dd, 1H, J = 13.6, J = 8.2), 4.59 (dd, 1H, J = 13.6, J = 4.2), 3.31 (br s, 1H). **^{13}C NMR** (100 MHz, $CDCl_3$, δ): 148.4, 140.3, 132.1, 130.0, 123.7, 121.1, 80.6, 69.8. **HRMS** (ESI^+): *m/z* $[M + Na]^+$ calculated for $C_8H_8N_2NaO_5$ 235.0326, found 235.0322.

*2-Nitro-1-(3-nitrophenyl)ethan-1-one (**3**)*. To a solution of **2** (891 mg, 4.20 mmol) in acetone (11 mL) cooled to 0 °C, Jones reagent* (2.2 mL, 4.83 mmol) was added. The addition was done slowly during the first 30 min until the orange colour persisted and, at such time, the remaining volume was added. The reaction mixture was stirred at 0 °C for 1 h. Then, Jones reagent (2.2 mL, 4.83 mmol) was added again and the reaction mixture was stirred at room temperature for 2 additional hours. The excess of oxidant was quenched with isopropanol (5.0 mL) and the resulting mixture was diluted with distilled water (10 mL) and extracted with dichloromethane (2 × 15 mL). The combined organic phases were dried with anhydrous $MgSO_4$, filtered and evaporated under reduced pressure. The resulting residue was washed with diisopropyl ether to afford compound **3** (776 mg, 88% yield) as a white solid. **Mp**: 94–95 °C. **IR** (KBr, ν_{max}/cm^{-1}): 1331, 1358, 1522, 1563, 1717. **^{1}H NMR** (400 MHz, acetone-d_6, δ): 8.80–8.77 (m, 1H), 8.58 (ddd, 1H, J = 8.0, J = 2.0, J = 0.8), 8.45 (ddd, 1H, J = 7.6, J = 1.6, J = 0.8), 7.95 (ddd, 1H, J = 8.0, J = 7.6, J = 0.4), 6.54 (s, 2H). **^{13}C NMR** (100 MHz, acetone-d_6, δ): 187.4, 149.5, 136.0, 135.0, 131.6, 129.6, 123.9, 83.0. **HRMS** (ESI^+): *m/z* $[M + Na]^+$ calculated for $C_8H_6N_2NaO_5$ 233.0169, found 233.0175.

* Jones reagent was prepared by dissolving CrO_3 (1.09 g, 10.90 mmol) and H_2SO_4 (1.0 mL) in 4 mL of distilled water.

*6-(3-Nitrophenyl)-2-oxo-4-(trifluoromethyl)-1,2-dihydropyridine-3-carbonitrile (**6**)*. To a mixture of *m*-nitroacetophenone (4.95 g, 30.0 mmol) and ethyl trifluoroacetate (10.7 mL, 90.0 mmol) in methanol (100 mL), a 30% solution of sodium methoxide in methanol (10.8 mL, 60.0 mmol) was added dropwise and the resulting solution was stirred for 16 h at room temperature. Then, the reaction mixture was acidified with 1 M HCl aqueous solution (150 mL) and extracted with dichloromethane (3 × 50 mL). The combined organic phases were dried with anhydrous $MgSO_4$, filtered and evaporated under reduced pressure to give intermediate compound **5** (7.63 g), which was used in the next step without further purification. To a mixture of crude product **5** (7.63 g) and cyanoacetamide (2.29 g, 27.2 mmol) in ethanol (27 mL), piperidine (0.27 mL, 2.72 mmol) was added dropwise and the reaction mixture was refluxed for 20 h. The reaction mixture was allowed to cool at room temperature and then introduced in an ice bath. The precipitate was collected by filtration, washed with cold ethanol (25 mL) and dried under vacuum to afford compound **6** (3.90 g, 42% yield) as a pale-yellow solid. **Mp**: 263–264 °C (decomposed). **IR** (KBr, ν_{max}/cm^{-1}): 1354, 1537, 1665, 2230. **^{1}H NMR** (400 MHz, acetone-d_6, δ): 8.92 (dd, 1H, J = 2.0, J = 1.6), 8.56 (ddd, 1H, J = 7.6, J = 1.6, J = 0.8), 8.44 (ddd, 1H, J = 8.0, J = 2.0, J = 0.8), 7.89 (dd, 1H, J = 8.0, J = 7.6), 7.76 (s, 1H). **^{13}C NMR** (100 MHz, acetone-d_6, δ): 164.2, 156.3, 149.8, 146.2 (q, J = 33), 136.9, 134.6, 131.5, 126.7, 123.5, 122.5 (q, J = 273), 113.1, 107.2, 95.7. **^{19}F NMR** (376 MHz, acetone-d_6, δ): −64.8. **HRMS** (ESI^+): *m/z* $[M + Na]^+$ calculated for $C_{13}H_6F_3N_3NaO_3$ 332.0253, found 332.0251.

*5-Nitro-6-(3-nitrophenyl)-2-oxo-4-(trifluoromethyl)-1,2-dihydropyridine-3-carbonitrile (**SynuClean-D**)*. To a solution of **6** (3.86 g, 12.5 mmol) in concentrated H_2SO_4 (60 mL) at 0 °C, cold fuming HNO_3 (25 mL) was added dropwise. The reaction mixture was stirred for 30 min at 0 °C and for additional 2 h at room temperature. Then, the reaction mixture was cooled in an ice bath and quenched by slow addition of cold distilled water (300 mL). The obtained precipitate was collected by filtration, washed with cold water and dried under vacuum to afford **SynuClean-D** (4.11 g, 93% yield) as a white solid. **Mp**: 255–256 °C (decomposed). **IR** (KBr, ν_{max}/cm^{-1}): 1341, 1355, 1533, 1545, 1668, 2236. **^{1}H NMR** (400 MHz, acetone-d_6, δ): 8.54 (ddd, 1H, J = 2.4, J = 1.6, J = 0.4), 8.50 (ddd, 1H, J = 8.4, J = 2.4, J = 1.2), 8.07 (ddd, 1H, J = 7.6, J = 1.6, J = 1.2), 7.92 (ddd, 1H, J = 8.4, J = 7.6, J = 0.4). **^{13}C NMR** (100 MHz, acetone-d_6, δ): 161.4, 150.9, 149.2, 139.0 (q, J = 34), 134.9, 133.6, 132.9, 131.7, 127.1, 124.3, 121.0 (q, J = 275), 112.0, 101.1. **^{19}F NMR** (376 MHz, acetone-d_6, δ): −62.3. **HRMS** (ESI^+): *m/z* $[M + Na]^+$ calculated for $C_{13}H_5F_3N_4NaO_5$ 377.0104, found 377.0102.

*6-(3-Cyanophenyl)-2-oxo-4-(trifluoromethyl)-1,2-dihydropyridine-3-carbonitrile (**8a**)*. To a mixture of *m*-cyanoacetophenone (435 mg, 3.00 mmol) and ethyl trifluoroacetate (1.1 mL, 9.00 mmol) in methanol (10 mL), a 30% solution of sodium methoxide in methanol (1.1 mL, 6.00 mmol) was added dropwise and the resulting solution was stirred for 16 h at room temperature. Then, the reaction mixture was acidified with 1 M HCl aqueous solution (15 mL) and extracted with dichloromethane (3 × 10 mL). The combined organic phases were dried with anhydrous $MgSO_4$, filtered and evaporated under reduced pressure to give intermediate compound **7a** (640 mg), which was used in the next step without further purification. To a mixture of crude product **7a** (640 mg) and cyanoacetamide (198 mg, 2.36 mmol) in ethanol (2.4 mL), piperidine (23.7 μL, 0.24 mmol) was added dropwise and the reaction mixture was refluxed for 20 h. The reaction mixture was cooled to room temperature and then introduced in an ice bath. The precipitate was collected by filtration, washed with cold ethanol and dried under vacuum to afford compound **8a** (203 mg, 23% yield) as a light-yellow solid. **Mp**: 298–299 °C. **IR** (KBr, ν_{max}/cm^{-1}): 1649, 2234. **^{1}H NMR** (400 MHz, acetone-d_6, δ): 8.51 (ddd, 1H, J = 2.0, J = 1.2, J = 0.4), 8.42 (ddd, 1H, J = 8.0, J = 2.0, J = 1.2), 8.01 (ddd, 1H, J = 7.6, J = 1.2, J = 1.2), 7.82 (ddd, 1H, J = 8.0, J = 7.6, J = 0.4), 7.62 (s, 1H). **^{13}C NMR** (100 MHz, acetone-d_6, δ): 163.6, 156.0, 146.5 (q, J = 33), 136.1, 135.6, 132.9, 132.4, 131.2, 122.5 (q, J = 274), 118.6, 114.3, 113.2, 106.2, 96.4. **^{19}F NMR** (376 MHz, acetone-d_6, δ): −66.2. **HRMS** (ESI^+): *m/z* $[M + Na]^+$ calculated for $C_{14}H_6F_3N_3NaO$ 312.0355, found 312.0345.

*6-(3,5-Difluorophenyl)-2-oxo-4-(trifluoromethyl)-1,2-dihydropyridine-3-carbonitrile (**8b**)*. To a mixture of 3′,5′-difluoroacetophenone (468 mg, 3.00 mmol) and ethyl trifluoroacetate (1.1 mL, 9.00 mmol) in methanol (10 mL), a 30% solution of sodium methoxide in methanol (1.1 mL, 6.00 mmol) was added dropwise and the resulting solution was stirred for 16 h at room temperature. Then, the reaction mixture was acidified with 1 M HCl aqueous solution (15 mL) and extracted with dichloromethane (3 × 10 mL). The combined organic phases were dried with anhydrous $MgSO_4$, filtered and evaporated under reduced pressure to give intermediate compound **7b** (715 mg), which was used in the next step without further purification. To a mixture of crude product **7b** (715 mg) and cyanoacetamide (239 mg, 2.84 mmol) in ethanol (2.8 mL), piperidine (27.7 μL, 0.28 mmol) was added dropwise and the reaction mixture was refluxed for 20 h. The reaction mixture was cooled to room temperature and then introduced in an ice bath for 30 min. The precipitate was collected by filtration, washed with cold ethanol and dried under

vacuum to afford compound **8b** (411 mg, 46% yield) as a yellow solid. **Mp**: 251–252 °C. **IR** (KBr, ν_{max}/cm^{-1}): 1668, 2227. **^{1}H NMR** (400 MHz, acetone-d_6, δ): 7.85–7.75 (m, 2H), 7.64 (s, 1H), 7.28 (tt, 1H, J = 8.8, J = 2.4). **^{13}C NMR** (100 MHz, acetone-d_6, δ): 164.2 (dd, 2C, J = 246, J = 13), 163.9, 155.7, 146.3 (q, 1C, J = 33), 138.5 (t, 1C, J = 10), 122.4 (q, 1C, J = 273), 113.1, 111,9 (dd, 2C, J = 20, J = 7.8), 107.4 (t, 1C, J = 26), 106.9, 96.2. **^{19}F NMR** (376 MHz, acetone-d_6, δ): −66.1, −111.0. **HRMS** (ESI^+): *m/z* $[M + Na]^+$ calculated for $C_{13}H_5F_5N_2NaO$ 323.0214, found 323.0207.

*6-(3-Bromophenyl)-2-oxo-4-(trifluoromethyl)-1,2-dihydropyridine-3-carbonitrile (**8c**)*. To a mixture of *m*-bromoacetophenone (399 μL, 3.00 mmol) and ethyl trifluoroacetate (1.1 mL, 9.00 mmol) in methanol (10 mL), a 30% solution of sodium methoxide in methanol (1.1 mL, 6.00 mmol) was added dropwise and the resulting solution was stirred for 16 h at room temperature. Then, the reaction mixture was acidified with 1 M HCl aqueous solution (15 mL) and extracted with dichloromethane (3 × 10 mL). The combined organic phases were dried with anhydrous $MgSO_4$, filtered and evaporated under reduced pressure to give intermediate compound **7c** (885 mg), which was used in the next step without further purification. To a mixture of crude product **7c** (885 mg) and cyanoacetamide (230 mg, 2.73 mmol) in ethanol (2.7 mL), piperidine (26.7 μL, 0.27 mmol) was added dropwise and the reaction mixture was refluxed for 20 h. The reaction mixture was cooled to room temperature and then introduced in an ice bath. The precipitate was collected by filtration, washed with cold ethanol and dried under vacuum to afford compound **8c** (524 mg, 51% yield) as a yellow solid. **Mp**: 234–235 °C. **IR** (KBr, ν_{max}/cm^{-1}): 1652, 2232. **^{1}H NMR** (400 MHz, acetone-d_6, δ): 8.25 (ddd, 1H, J = 2.0, J = 2.0, J = 0.4), 8.07 (ddd, 1H, J = 8.0, J = 2.0, J = 0.8), 7.80 (ddd, 1H, J = 8.0, J = 2.0, J = 0.8), 7.55 (ddd, 1H, J = 8.0, J = 8.0, J = 0.4), 7.45 (s, 1H). **^{13}C NMR** (100 MHz, acetone-d_6, δ): 163.1, 155.9, 146.7 (q, J = 33), 136.5, 135.4, 131.9, 131.5, 127.6, 123.6, 122.4 (q, J = 273), 113.3, 105.2, 97.1. **^{19}F NMR** (376 MHz, acetone-d_6, δ): −66.2. **HRMS** (ESI^+): *m/z* $[M + Na]^+$ calculated for $C_{13}H_6BrF_3N_2NaO$ 364.9508, found 364.9496.

*6-(3,5-Dibromophenyl)-2-oxo-4-(trifluoromethyl)-1,2-dihydropyridine-3-carbonitrile (**8d**)*. To a mixture of 3′,5′-dibromoacetophenone (834 mg, 3.00 mmol) and ethyl trifluoroacetate (1.1 mL, 9.00 mmol) in methanol (10 mL), a 30% solution of sodium methoxide in methanol (1.1 mL, 6.00 mmol) was added dropwise and the resulting solution was stirred for 16 h at room temperature. Then, the reaction mixture was acidified with 1 M HCl aqueous solution (15 mL) and extracted with dichloromethane (3 × 10 mL). The combined organic phases were dried with anhydrous $MgSO_4$, filtered and evaporated under reduced pressure to give intermediate compound **7d** (1.07 g), which was used in the next step without further purification. To a mixture of crude product **7d** (1.07 g) and cyanoacetamide (240 mg, 2.85 mmol) in ethanol (2.8 mL), piperidine (27.7 μL, 0.28 mmol) was added dropwise and the reaction mixture was refluxed for 20 h. The reaction mixture was cooled to room temperature and then introduced in an ice bath. The precipitate was collected by filtration, washed with cold ethanol and dried under vacuum to afford compound **8d** (479 mg, 38% yield) as a yellow solid. **Mp**: 273–274 °C. **IR** (KBr, ν_{max}/cm^{-1}): 1674, 2234. **^{1}H NMR** (400 MHz, acetone-d_6, δ): 8.30 (d, 2H, J = 1.6), 7.98 (t, 1H, J = 1.6), 7.71 (s, 1H). **^{13}C NMR** (100 MHz, acetone-d_6, δ): 164.0, 155.4, 146.1 (q, J = 33), 138.8, 137.1, 130.5, 124.2, 122.5 (q, J = 273), 113.1, 107.1, 95.9. **^{19}F NMR** (376 MHz, acetone-d_6, δ): −66.0. **HRMS** (ESI^-): *m/z* $[M - H]^-$ calculated for $C_{13}H_4Br_2F_3N_2O$ 418.8648, found 418.8634.

*1-Methyl-2-oxo-6-phenyl-4-(trifluoromethyl)-1,2-dihydropyridine-3-carbonitrile (**8e**)*. To a mixture of benzoyl-1,1,1-trifluoroacetone **7e** (216 mg, 1.00 mmol) and 2-cyano-*N*-methyl-acetamide (98 mg, 1.00 mmol) in ethanol (1.0 mL), piperidine (9.9 μL, 0.1 mmol) was added dropwise and the reaction mixture was refluxed for 20 h. The reaction mixture was cooled to room temperature and evaporated under reduced pressure. The resulting residue was purified by column chromatography (eluent 1: Et_2O/hexane 1:1, eluent 2: Et_2O) to afford compound **8e** (182 mg, 65% yield) as a white solid. **Mp**: 129–130 °C. **IR** (KBr, ν_{max}/cm^{-1}): 1651, 2227. **^{1}H NMR** (400 MHz, $CDCl_3$, δ): 7.63–7.52 (m, 3H), 7.41–7.36 (m, 2H), 6.43 (s, 1H), 3.50 (s, 3H). **^{13}C NMR** (100 MHz, $CDCl_3$, δ): 160.3, 157.1, 145.2 (q, J = 34), 133.1, 131.0, 129.2, 127.8, 120.7 (q, J = 275), 112.4, 103.4 (q, J = 4.2), 99.5, 35.8. **^{19}F NMR** (376 MHz, $CDCl_3$, δ): −64.7. **HRMS** (ESI^+): *m/z* $[M + Na]^+$ calculated for $C_{14}H_9F_3N_2NaO$ 301.0559, found 301.0557.

*1-Methyl-6-(3-nitrophenyl)-2-oxo-4-(trifluoromethyl)-1,2-dihydropyridine-3-carbonitrile (**8f**)*. To a mixture of *m*-nitroacetophenone (495 mg, 3.00 mmol) and ethyl trifluoroacetate (1.1 mL, 9.00 mmol) in methanol (10 mL), a 30% solution of sodium methoxide in methanol (1.1 mL, 6.00 mmol) was added dropwise and the resulting solution was stirred for 16 h at room temperature. Then, the reaction mixture was acidified with 1 M HCl aqueous solution (15 mL) and extracted with dichloromethane (3 × 10 mL). The combined organic phases were dried with anhydrous $MgSO_4$, filtered and evaporated under reduced pressure to give intermediate compound **7f** (763 mg), which was used in the next step without further purification. To a mixture of crude product **7f** (763 mg) and 2-cyano-*N*-methyl-acetamide (267 mg, 2.72 mmol) in ethanol (2.7 mL), piperidine (26.7 μL, 0.27 mmol) was added dropwise and the reaction mixture was refluxed for 20 h. The reaction mixture was cooled to room temperature and evaporated under reduced pressure. The resulting residue was dissolved in dichloromethane (15 mL) and washed with distilled water (2 × 10 mL). The organic phase was dried with anhydrous $MgSO_4$, filtered and evaporated under reduced pressure. The resulting residue was purified by column chromatography (eluent 1: Et_2O/hexane 4:1, eluent 2: Et_2O) to afford compound **8f** (345 mg, 36% yield) as a white solid. **Mp**: 207–208 °C. **IR** (KBr, ν_{max}/cm^{-1}): 1350, 1537, 1667, 2232. **^{1}H NMR** (400 MHz, acetone-d_6, δ): 8.55 (ddd, 1H, J = 2.4, J = 1.6, J = 0.4), 8.49 (ddd, 1H, J = 8.4, J = 2.4, J = 0.8), 8.14 (ddd, 1H, J = 8.0, J = 1.6, J = 0.8), 7.95 (ddd, 1H, J = 8.4, J = 8.0, J = 0.4), 6.77 (s, 1H), 3.51 (s, 3H). **^{13}C NMR** (100 MHz, acetone-d_6, δ): 160.9, 156.3, 149.4, 145.7 (q, J = 33), 136.1, 135.5, 131.6, 126.1, 124.6, 122.2 (q, J = 274), 113.6, 104.2 (q, J = 4.3), 100.8, 36.1. **^{19}F NMR** (376 MHz, acetone-d_6, δ): −66.6. **HRMS** (ESI^+): *m/z* $[M + Na]^+$ calculated for $C_{14}H_8F_3N_3NaO_3$ 346.0410, found 346.0405.

*1-Methyl-5-nitro-6-(3-nitrophenyl)-2-oxo-4-(trifluoromethyl)-1,2-dihydropyridine-3-carbonitrile (**9**)*. Fuming HNO_3 (0.40 mL) was cooled and added dropwise to a solution of **8f** (65 mg, 0.20 mmol) in concentrated H_2SO_4 (1.0 mL) at 0 °C. The reaction mixture was stirred for 30 min at 0 °C and for additional 2 h at room temperature. Then, the reaction mixture was cooled in an ice bath and quenched by slow addition of cold distilled water (4 mL). The obtained precipitate was collected by filtration, washed with cold water and dried under vacuum to afford compound **9** (53 mg, 72% yield) as a white solid. **Mp**: 91–92 °C. **IR** (KBr, ν_{max}/cm^{-1}): 1352, 1536, 1684, 2238. **^{1}H NMR** (400 MHz, acetone-d_6, δ): 8.58–8.53 (m, 2H), 8.11–8.06 (m, 1H), 8.04–7.98 (m, 1H), 3.42 (s, 3H). **^{13}C NMR** (100 MHz, acetone-d_6, δ): 159.1, 151.0, 149.5, 138.4 (q, J = 34), 135.3, 132.2, 131.6, 130.7, 127.3, 124.5, 120.9 (q, J = 276), 112.4, 103.8, 36.7. **^{19}F NMR** (376 MHz, acetone-d_6, δ): −62.7. **HRMS** (ESI^+): *m/z* $[M + Na]^+$ calculated for $C_{14}H_7F_3N_4NaO_5$ 391.0261, found 391.0247.

4.6. Structure-activity analysis

The structure-activity analysis was done by breaking down the differential effects observed in the aggregative inhibitory activity for the nine **SynuClean-D** derivatives described (obtained by subtracting SynuClean-D's aggregative inhibitory potency from those of the derivatives). In practice, we sought to estimate the individual quantitative contributions by the functional groups added/removed to/from **SynuClean-D**. Contribution of a moiety was assumed to be positive when it is added to any sub-structure and negative when it is removed. The equations derived and the individual quantitative contributions obtained are presented in Table 3 and Fig. 7. Compound **1**, displaying the atypical effect of reinforcing the aggregation, was considered as an outlier and was not included in the quantitative analysis.

Declaration of Competing Interest

The authors declare that they have no known competing financial interests or personal relationships that could have appeared to influence the work reported in this paper.

Acknowledgements

This research was funded by Spanish Ministry of Science and Innovation (grants PID2019-107293GB-I00 to JS and PID2019-105017RB-I00 to SV), by Gobierno de Aragón, Spain (grants LMP30_18 and E45_20R to JS), by ICREA (ICREA-Academia 2015 to SV) and by "la Caixa" Banking Foundation, Spain (grant CaixaImpulse CI18-00019, to SV). AM was a recipient of a predoctoral FPU fellowship from the Spanish Government.

Appendix A. Supplementary data

Supplementary data to this article can be found online at https://doi.org/10.1016/j.bioorg.2021.105472.

References

[1] E.R. Dorsey, T. Sherer, M.S. Okun, B.R. Bloem, P. Brundin, J.W. Langston, B. R. Bloem, The emerging evidence of the Parkinson pandemic, J. Parkinsons. Dis. 8 (s1) (2018) S3–S8.
[2] M. Goedert, Alpha-synuclein and neurodegenerative diseases, Nat. Rev. Neurosci. 2 (7) (2001) 492–501.
[3] L.V. Kalia, A.E. Lang, Parkinson's disease, Lancet 386 (9996) (2015) 896–912.
[4] A.H.V. Schapira, K.R. Chaudhuri, P. Jenner, Non-motor features of Parkinson disease, Nat. Rev. Neurosci. 18 (7) (2017) 435–450.
[5] P.A. Lewis, J.E. Spillane, Chapter 3: Parkinson's disease, in: Mol. Clin. Pathol. Neurodegener. Dis., First Edit, Academic Press, 2019: pp. 83–121.
[6] R.G. Perez, Editorial: The protein alpha-synuclein: its normal role (in neurons) and its role in disease, Front. Neurosci. 14 (2020) 116.
[7] H. Deng, P. Wang, J. Jankovic, The genetics of Parkinson disease, Ageing Res. Rev. 42 (2018) 72–85.
[8] E. Valera, E. Masliah, Therapeutic approaches in Parkinson's disease and related disorders, J. Neurochem. 139 (2016) 346–352.
[9] N. Cremades, A. Velázquez-Campoy, M. Martínez-Júlvez, J.L. Neira, I. Pérez-Dorado, J. Hermoso, P. Jiménez, A. Lanas, P.S. Hoffman, J. Sancho, Discovery of specific flavodoxin inhibitors as potential therapeutic agents against Helicobacter pylori infection, ACS Chem. Biol. 4 (11) (2009) 928–938.
[10] L.C. López, S. Dos-Reis, A. Espargaró, J.A. Carrodeguas, M.L. Maddelein, S. Ventura, J. Sancho, Discovery of novel inhibitors of amyloid beta-peptide 1–42 aggregation, J. Med. Chem. 55 (2012) 9521–9530.
[11] J. Pujols, S. Peña-Díaz, M. Conde-Giménez, F. Pinheiro, S. Navarro, J. Sancho, S. Ventura, High-throughput screening methodology to identify alpha-synuclein aggregation inhibitors, Int. J. Mol. Sci. 18 (2017) 478.
[12] J. Pujols, S. Peña-Díaz, D.F. Lázaro, F. Peccati, F. Pinheiro, D. González, A. Carija, S. Navarro, M. Conde-Giménez, J. García, S. Guardiola, E. Giralt, X. Salvatella, J. Sancho, M. Sodupe, T.F. Outeiro, E. Dalfó, S. Ventura, Small molecule inhibits α-synuclein aggregation, disrupts amyloid fibrils, and prevents degeneration of dopaminergic neurons, Proc. Natl. Acad. Sci. 115 (41) (2018) 10481–10486.
[13] S. Peña-Díaz, J. Pujols, M. Conde-Giménez, A. Čarija, E. Dalfo, J. García, S. Navarro, F. Pinheiro, J. Santos, X. Salvatella, J. Sancho, S. Ventura, ZPD-2, a small compound that inhibits α-synuclein amyloid aggregation and its seeded polymerization, Front. Mol. Neurosci. 12 (2019) 306.
[14] S. Peña-Díaz, J. Pujols, F. Pinheiro, J. Santos, I. Pallarés, S. Navarro, M. Conde-Gimenez, J. García, X. Salvatella, E. Dalfó, J. Sancho, S. Ventura, Inhibition of α-synuclein aggregation and mature fibril disassembling with a minimalistic compound, ZPDm, Front. Bioeng. Biotechnol. 8 (2020), 588947.
[15] W.M. Pardridge, The blood-brain barrier: Bottleneck in brain drug development, NeuroRx. 2 (2005) 3–14.
[16] Z. Rankovic, CNS drug design: balancing physicochemical properties for optimal brain exposure, J. Med. Chem. 58 (2015) 2584–2608.
[17] S.A. Hitchcock, L.D. Pennington, Structure-brain exposure relationships, J. Med. Chem. 49 (26) (2006) 7559–7583.
[18] S. Portnoy, Fluorinated nitrogen heterocycles via cyclization. I. Trifluoromethyl-2-pyridones from fluorinated 1,3-dicarbonyls and cyanoacetamide, J. Org. Chem. 30 (10) (1965) 3377–3380.
[19] B. Narsaiah, A. Sivaprasad, R.V. Venkataratnam, An improved synthetic route to trifluoromethyl-6-substituted-2(1H)-pyridones, Org. Prep. Proced. Int. 25 (1) (1993) 116–117.
[20] K. Aradi, Á. Mészáros, B.L. Tóth, Z. Vincze, Z. Novák, Copper-catalyzed N-arylation of nitroenamines with diaryliodonium salts, J. Org. Chem. 82 (22) (2017) 11752–11764.
[21] C. Liu, Z. Cui, X. Yan, Z. Qi, M. Ji, X. Li, Synthesis, fungicidal activity and mode of action of 4-phenyl-6-trifluoromethyl-2-aminopyrimidines against Botrytis cinerea, Molecules 21 (2016) 828.
[22] M. Kruszyk, M. Jessing, J.L. Kristensen, M. Jørgensen, Computational methods to predict the regioselectivity of electrophilic aromatic substitution reactions of heteroaromatic systems, J. Org. Chem. 81 (12) (2016) 5128–5134.
[23] J.C. Kromann, J.H. Jensen, M. Kruszyk, M. Jessing, M. Jørgensen, Fast and accurate prediction of the regioselectivity of electrophilic aromatic substitution reactions, Chem. Sci. 9 (3) (2018) 660–665.
[24] J.L. Greene, J.A. Montgomery, Vitamin B6 analogs. II. Synthesis of 4,6-dimethyl-5-mercapto-3-pyridinemethanol and of 5-mercapto-6-methyl-3,4-pyridinedimethanol hydrochlorides, J. Med. Chem. 7 (1964) 17–20.
[25] A. Daina, V. Zoete, A BOILED-Egg to predict gastrointestinal absorption and brain penetration of small molecules, ChemMedChem 11 (11) (2016) 1117–1121.
[26] H. Liu, L. Wang, M. Lv, R. Pei, P. Li, Z. Pei, Y. Wang, W. Su, X.Q. Xie, AlzPlatform: An Alzheimer's disease domain-specific chemogenomics knowledgebase for polypharmacology and target identification research, J. Chem. Inf. Model. 54 (2014) 1050–1060.
[27] Y.H. Zhao, M.H. Abraham, A. Ibrahim, P.V. Fish, S. Cole, M.L. Lewis, M.J. de Groot, D.P. Reynolds, Predicting penetration across the blood-brain barrier from simple descriptors and fragmentation schemes, J. Chem. Inf. Model. 47 (1) (2007) 170–175.
[28] A. Pedretti, A. Mazzolari, S. Gervasoni, L. Fumagalli, G. Vistoli, The VEGA suite of programs: an versatile platform for cheminformatics and drug design projects, Bioinformatics. btaa774 (2020).
[29] A. Daina, O. Michielin, V. Zoete, SwissADME: A free web tool to evaluate pharmacokinetics, drug-likeness and medicinal chemistry friendliness of small molecules, Sci. Rep. 7 (2017) 42717.
[30] V. Purohit, A.K. Basu, Mutagenicity of nitroaromatic compounds, Chem. Res. Toxicol. 13 (8) (2000) 673–692.
[31] R. Crespo, E. Villar-Alvarez, P. Taboada, F.A. Rocha, A.M. Damas, P.M. Martins, What can the kinetics of amyloid fibril formation tell about off-pathway aggregation?, J. Biol. Chem. 291 (2016) 2018–2032.